



## Research article

## *In silico* analysis and transcript levels of non-specific lipid transfer proteins (SiLTPI.5 and SiLTPII.1) under abiotic stresses in sesame (*Sesamum indicum*)

Supaporn Baiya<sup>a,\*</sup>, Sunan Kitjaruwankul<sup>b</sup>, Methee Juntaropakorn<sup>a</sup>, Malinee Promkatkaew<sup>b</sup>

<sup>a</sup> Department of Resources and Environment, Faculty of Science at Sriracha, Kasetsart University, Sriracha Campus, Chonburi 20230, Thailand

<sup>b</sup> Department of Fundamental Science and Physical Education, Faculty of Science at Sriracha, Kasetsart University, Sriracha Campus, Chonburi 20230, Thailand

### Article Info

#### Article history:

Received 3 April 2023

Revised 18 September 2023

Accepted 29 September 2023

Available online 31 October 2023

#### Keywords:

Docking,

Molecular dynamics simulations,

Plant non-specific lipid transfer protein (nsLTPIs),

Quantitative real-time polymerase chain reaction (qRT-PCR),

*Sesamum indicum*

### Abstract

**Importance of the work:** Non-specific lipid transfer proteins are found in all land plants; however, there have been no published articles on computational analysis or gene expression under different abiotic stresses of sesame (*Sesamum indicum*).

**Objectives:** To demonstrate the ligand-binding interaction of lipid molecules with the proteins of SiLTPI.5 and SiLTPII.1 and to examine the transcript levels of these corresponding genes in response to salt, chilling, heating, salicylic acid and abscisic acid.

**Materials & Methods:** The spatial structures of SiLTPI.5 and SiLTPII.1 were simulated using the SWISS-MODEL server. Then, molecular docking of these modeled structures with 22 ligands was executed and molecular dynamics (MD) simulations of the docked protein-ligand complex (SiLTPIs-[ergo]sterol) were completed. Quantitative real-time polymerase chain reaction of *SiLTPIs* under abiotic stress was carried out using gene-specific primers.

**Results:** The overall structure of SiLTPI.5 consisted of four helices, four loops and a long C-terminal with a  $3_{10}$ -helix. SiLTPII.1 consisted of five helices, an N-terminal  $3_{10}$ -helix and a C-terminal with a short polyproline type II. SiLTPI.5 and SiLTPII.1 with  $\Delta G$  values of -6.92 kcal/mol and -6.87 kcal/mol, respectively, could likely bind with (ergo)sterol rather than other lipid molecules. The MD simulations confirmed that the SiLTPIs-ligand complexes were maintained and stabilized via hydrophobic force and hydrogen bonding. Finally, the *SiLTPI.5* and *SiLTPII.1* genes were significantly regulated after abiotic treatments.

**Main finding:** The SiLTPI-lipids interactions were stabilized via conserved amino acid with hydrophobic side chains around the binding region, together with some hydrogen bonds between the protein and ligand. The *SiLTPI.5* and *SiLTPII.1* genes play a crucial role in stress responses.

\* Corresponding author.

E-mail address: [Supaporn.bai@ku.th](mailto:Supaporn.bai@ku.th) (S. Baiya)

online 2452-316X print 2468-1458/Copyright © 2023. This is an open access article under the CC BY-NC-ND license (<http://creativecommons.org/licenses/by-nc-nd/4.0/>), production and hosting by Kasetsart University Research and Development Institute on behalf of Kasetsart University.

<https://doi.org/10.34044/j.anres.2023.57.5.05>

## Introduction

*Sesamum indicum* is the queen of oilseed due to its high nutritional value, with several health benefits, which have enhanced worldwide consumption (Ma et al., 2022). Sesamin and sesamol, two distinct compounds found in the seed, are responsible for a wide range of pharmacological activity, such as antioxidative, anti-carcinogenic, anti-inflammatory, anti-proliferative, anti-hypertensive, and anti-melanogenesis effects (Khuimphukhieo et al., 2020; Dossou et al., 2023). In addition, sesame has efficacy as an adjuvant therapeutic agent for the treatment of hyperlipidemia and related morbidities which avoids the harmful hepatotoxic side effects related to the usage of commonly prescribed blood lipid-lowering medications (Adeyanju et al., 2022). Because of their benefits, sesame seeds are highly valued in the confectionery and baking industry sectors, as well as for other culinary specialties, such as snacks, cookies and fermented foods like soybean and peanut (Namiki, 2007). However, sesame is sensitive to environmental stresses. As a result, the primary goal of sesame breeding is to produce environmentally stable sesame cultivars with high oil and nutrition contents.

Both biotic and abiotic factors can directly or indirectly hamper plant growth and productivity, with drought, salinity, heat, chilling, freezing, ozone and radiation being the dominant cues of primary abiotic stresses that restrict crop productivity (Wani et al., 2016). It has been stated that stress induced by drought and salinity causes oxidative stress by increasing reactive oxygen species (ROS), resulting in damage to the membranes, proteins, nucleic acids, and lipids of cells (Gupta et al., 2022). Heat stresses may adversely affect membrane stability and cause increased permeability and leakage of ions (Wahid et al., 2007). Furthermore, chilling injury was increased by the leakage of the cell contents from plant tissues, leading to the loss of water from cells and thus, a decrease in tissue fresh weight (Korkmaz et al., 2021). However, plants have diverse and complicated mechanisms to respond to and tolerate various environmental stresses (Qin et al., 2011). For example, salinity stress in ROS-damaged plants strongly affected both plant primary (carbohydrates, amino acid and nitrogen) and secondary (defense compounds) metabolites and negatively affected protein biosynthesis and ion absorption (Ma et al., 2020). In addition, Hairat et al. (2018) found that lipid transfer proteins played roles in repairing stress-induced damage in membranes.

Non-specific lipid transfer proteins (nsLTPs) are found in many species of land plants and they are defined according to their ability to associate with various phospholipids and to

have non-specific binding to different lipids (Østergaard et al., 1993; Carvalho and Gomes, 2007; Liu et al., 2015). Several clues have indicated that nsLTPs are involved in plant tolerance to biotic and abiotic stresses (Missouai et al., 2022). The transcription levels of nsLTPs in many plant species, as well as in different nsLTP isoforms, varied in response to different abiotic stresses, such as drought, salinity, heat and cold (Liu et al., 2015). In addition, a difference in signaling molecules, such as abscisic acid (ABA), salicylic acid (SA), indole acetic acid, methyl jasmonic acid, gibberellic acid (GA) and ethylene, induces the expression profiles of nsLTPs (Wang et al., 2014; Safi et al., 2015; Gangadhar et al., 2016; Chen et al., 2017; Akhiyarova et al., 2020; Yang et al., 2022; Zhang et al., 2022).

Plant nsLTPs are small proteins, usually 6.5–10.5 kDa, that are stabilized with four conserved disulfide bridges. The common form of the eight-cysteine motif (C-Xn-C-Xn-CC-Xn-CXC-Xn-C-Xn-C) contributes to the 3D structure of the four- $\alpha$ -helix fold, giving a formation of a hydrophobic tunnel-like cavity (Salminen et al., 2016; Cuevas-Zuñiría et al., 2019). The cavity in nsLTPI is larger than in nsLTPII, promoting greater flexibility to accommodate single or double-chain lipids and rigid ligands, including sterols (Finkina et al., 2016; Scheurer and Schülke, 2018). An *in vitro* study of LcLTPII from *Lens culinaris* seeds revealed the ability of the protein to bind different saturated fatty acid lengths of C12–C22, unsaturated fatty acids with chain lengths of C16–C22, jasmonic acid (JA) and lysolipids (Shenkarev et al., 2017). Despite, the isolation of natural ligands purified from peach peel, mugwort pollen, pellitory pollen and olive pollen, they only carried individual-specific ligands (Cubells-Baeza et al., 2017; Gonzalez-Klein et al., 2021), suggesting that biological preferential ligands are highly limited. The accession of a ligand into the tunnel cavity seems to rely on the nsLTP, so that a similar ligand could be exhibited in the opposite orientation based on the bonding interactions (Cheng et al., 2004a; Melnikova et al., 2020).

Since nsLTPs are encoded as complex different isoforms in multigenic families, their classification standard is constantly being re-established. Boutrot et al. (2008) classified nsLTP members in *Oryza sativa*, *Triticum aestivum* and *Arabidopsis thaliana* into nine types (I–IX), based on sequence similarity and the number of amino acid residues between the eight-cysteine motif (ECM). Nonetheless, this classification criterion did not cover non-flowering plants. Notably, the classification of nsLTPs evolved according to revisions of the plant classification system. The new classification system based on intron positions, the presence of glycosylphosphatidylinositol modification sites, cysteine spacing in the ECM and sequence

similarity has classified nsLTPs into 10 types: LTP1, LTP2, LTPc, LTPd, LTPe, LTPf, LTPg, LTPh, LTPj and LTPk (Edstam et al., 2011).

The expressed sequence tags (ESTs) acquired from a cDNA library of developing sesame seeds showed that LTPs were one of the omnipresent protein groups in sesame ESTs (Suh et al., 2003). Choi et al. (2008) isolated five LTP cDNAs from developing sesame seed ESTs and revealed that these sesame isoforms were significantly regulated by NaCl, mannitol, GA<sub>3</sub> and ABA. Based on genome-wide analysis of the *nsLTP* gene family in sesame, *SiLTPs* were identified and classified into nine types according to the criteria developed by Boutrot et al. (2008). Their ability to interact with multiple transcription factors, such as APETALA2 (AP2), and DNA binding with one finger (Dof) were observed. These interactions led to an increased lipid content in seeds (Song et al., 2021). Since LTPI and LTPII are the major types of nsLTP protein and reports have yet been published on computational analysis and gene expression under abiotic stress of sesame, modeling, docking, and dynamics simulations were proposed to demonstrate the ligand-binding interaction with the proteins of SiLTPI.5 and SiLTPII.1 as representatives of types I and II. Notably, these two subfamilies I and II present in 32 paralogs and 3 paralogs, respectively (Song et al., 2021). The current study aimed to examine the transcript levels of these corresponding genes in response to salt, chilling, heating, SA and ABA. The results may contribute to a better understanding of the specific mechanism of SiLTPs.

---

## Materials and Methods

### *Data preparation and homology modeling of SiLTPs*

The SiLTPI.5 (SIN\_1013882) and SiLTPII.1 (SIN\_1013701) protein sequences were downloaded from <https://plants.ensembl.org>. The signal peptide was predicted by the SignalP-5.0 server (<https://services.healthtech.dtu.dk/service.php?SignalP-5.0>). Then, homology modeling of the 3D structure of mature SiLTPI.5 and SiLTPII.1 was obtained using the SWISS-MODEL server (<https://swissmodel.expasy.org/>). The template search with BLAST and HHblits was performed against the SWISS-MODEL template library. Then, 50 and 30 templates were found for SiLTPI.5 and SiLTPII.1, respectively. A template of X-ray crystallography with high resolution, high global model quality estimate (GMQE), sequence similarity and coverage was selected to build a model. The structures of *Solanum melongena*, PDB code:

6IWM (Madni et al., 2020) and *Triticum aestivum*, PDB code: 1TUK (Hoh et al., 2005) were used as templates for SiLTPI.5 and SiLTPII.1, respectively. The amino acid multiple sequence alignment was generated using the MUSCLE algorithm implemented in the MEGA X software (Edgar, 2004).

### *Molecular docking*

Molecular docking was executed using Autodock 4.2 (ADT version 1.5.6; Baiya et al., 2021) to consider the interactions of SiLTPI.5 and SiLTPII.1 with 22 ligands that had been reported as potential ligands for nsLTP. The ligands were retrieved from the Protein Data Bank (<https://www.rcsb.org>). For protein preparation, polar hydrogen atoms and Kollman charges were added and the aromaticity criterion was set to 7.5. The ligands were docked into the proteins with a grid box dimension 60 points × 60 points × 60 points in the x, y and z axes and a grid spacing of 0.375 Å via a Lamarckian genetic algorithm methodology. The docking was run 100 times for each ligand using Cygwin (v.3.4.5) and the conformation which showed the best binding energy ( $\Delta G$ ) was selected (Rizvi et al., 2013).

### *Molecular dynamics simulations*

MD simulations of a docked protein-ligand complex (SiLTPs-[ergo]sterol) were completed using the NAMD software v.2.12 (Phillips et al., 2008). The CHARMM36m force field was used for the protein, whereas the force field of (ergo)sterol was computed from the charmm-gui server ([http://charmm-gui.org/?doc=license\\_cgui](http://charmm-gui.org/?doc=license_cgui)) (Huang et al., 2016). The PSF file was processed using Visual Molecular Dynamics v.1.9.4 (Humphrey et al., 1996). The docked system was solvated in cubic water boxes containing transferable intermolecular potential with 3-point (TIP3P) water molecules (Jorgensen et al., 1983). The size of a simulation box was set at a distance of 15 Å between the protein surface and the edges of the periodic box setting as 64 Å × 64 Å × 64 Å. SiLTPI.5 contained a total of 27,075 atoms with (ergo)sterol, while SiLTPII.1 contained a total of 23,661 atoms. The cut-off radius for nonbonded interactions was calculated at 12 Å. The particle mesh Ewald method was applied to calculate long-range electrostatic interactions (Darden et al., 1998). The SHAKE algorithm was applied to constrain all bonds involving hydrogen atoms (Ryckaert et al., 1977). The system was first minimized for 50,000 steps of steepest descent, then heated from 50 K to 300 K, while restraining the protein backbone and ligand molecule; after that, the protein

backbone and ligand molecule were continuously released and equilibrated at 300 K for 5 ns. The production MD run was performed using an NPT ensemble. The Nosé-Hoover method was used to maintain a constant temperature (Hoover, 1985). The simulation time step was set to 2 fs. The studied simulation time was 200 ns.

### Plant materials and treatments

Sesame seed genotypes CM-53 (white sesame) and CM-07 (black sesame) were provided by the Department of Agronomy, Kasetsart University, Bangkok, Thailand. The seeds were surface-sterilized in 1% sodium hypochlorite and then soaked in water overnight. Each soaked seed was transferred into a plastic nursery tray and cultured for 10 d. To assess the expression of the *SiLTPI.5* and *SiLTPII.1* genes under abiotic stresses, six treatments were carried out, including the control without abiotic stress treatment. There were 15 fifteen seedlings aged 10 d treated in each condition with NaCl (50 mM, 100 mM, 150 mM), chilling (4°C, 10°C, 15°C, 20°C), heating (37°C, 40°C, 45°C), and SA and ABA (both at 10 µM, 20 µM, 50 µM) (Safi et al., 2015; Chen et al., 2017). The seedlings at 30°C served as the control group for all five abiotic stress experiments. The treated sesame seedlings with chilling and heating were collected after 24 hr of treatment and the other stresses were collected after 5 d. The samples were immediately frozen in liquid nitrogen for RNA extraction. Each treatment condition contained three independent biological replicates and each replicate included at least two seedling samples.

### RNA extraction and quantitative real-time polymerase chain reaction

Total RNA was extracted using TRIzol reagent according to the manufacturer's protocol. The quality of RNA was determined by measuring the absorbances (A260 and A280) and running on agarose gel electrophoresis. The first-strand cDNA synthesis was reverse transcribed from the total RNA using Superscript™ III reverse transcriptase. The qRT-PCR was done following the manufacturer's protocol for the SYBR Green Mix (2x) with the gene-specific primers (*SiLTPI.5* fwd: 5'-GTGGATGCTGCTTTGGTTCC-3', *SiLTPI.5* rev: 5'-CACCACACTTGGTGGGAAGA-3', *SiLTPII.1* fwd: 5'-CACCGAATTCGTGACTTGC AACCCTGC-3', *SiLTPII.1* rev: 5'-GCGGCCGCGCATCTGGGGTATGGCGT-3') which were designed base on their mRNA sequence gene and the gene specificity was checked

using Primer-BLAST of the NCBI database. The product length for *SiLTPI.5* was 211 bp and for *SiLTPII.1* was 204 bp. The qRT-PCR reaction consisted of Luna Universal qPCR master mix (NEB: Ipswich, MA, USA), the gene-specific primer pair, first-strand cDNA and HPLC water to make up the reaction volume to 20 µL. After the qRT-PCR had finished, the qRT-PCR specificity was examined using 2% agarose gel and the relative gene expression ratios were calculated using the  $2^{-\Delta\Delta CT}$  method with 30°C seedling cDNA as the reference sample and actin (Fwd: 5'-GCTCCACCAGAG AGAAAGTACAG-3', Rev: 5'-GGAATCACGAGTTCCCTTTCATG-3') as the reference gene (Rao et al., 2013). The qRT-PCR was performed using a CFX96™ Real-Time System (Bio-Rad®, Hercules, Ca, USA). All experiments were done in biological triplicates.

### Statistical analysis

To validate the significant differences between the transcript quantities of the *SiLTPIs* genes under the different abiotic stress conditions of each gene for each genotype, statistical analysis was performed using one-way ANOVA with the post hoc Tukey's HSD test was performed in the IBM SPSS statistics software (version 21; IBM Corp.; Armonk, NY, USA). Significant differences among groups were considered at  $p < 0.05$ .

## Results and Discussion

### Overall structure of modeled *SiLTPIs*

*SiLTPI.5* contained 116 amino acid residues (a mature protein of 92 amino acids and a putative signal peptide of 24 amino acids), with pI of 8.12 and a mature mass of 9.39 kDa. SWISS-MODEL successfully simulated the 3D structure of *SiLTPI.5*, with a highest GMQE score of 0.87. Sequence comparison showed that *SiLTPI.5* was similar to the *S. melongena* nsLTP, with a sequence identity of 60.44% and a QMEANDisCo Global score of  $0.82 \pm 0.09$ . The quality of the constructed model assessed using a Ramachandran plot showed that 100% of the amino acids were in the most favorable allowed region with a MolProbity score of 0.86, indicating that the quality assessment of the homology modeling was reliable. Fig. 1A shows the nsLTP sequence alignments of known structures for *S. melongena* (a model template), *Actinidia chinensis* (PDB code: 7KSB; O'Malley et al., 2021), *Oryza sativa* (PDB code: 1UVC; Cheng et al., 2004b), *Zea mays* (PDB code: 1FK5; Han et al., 2001) and *Prunus persica* (PDB

code: 2B5S; Pasquato et al., 2006). The amino acid sequences shared significant similarities with ECM, with the highly conserved sequences shaded in black color. It has been reported that two consensus sequences (T/SXXDR/K and PYXIS) were provided as the region of lipid binding (Shi et al., 2013). The overall structure of SiLTPI.5 consisted of four helices, four loops, a long C-terminal with a  $3_{10}$ -helix and four disulfide bonds, as observed in other members of the nsLTPI family (Madni et al., 2020). A hydrophobic tunnel formation ran from the N-terminal through the C-terminal, appearing as a closed cavity form (Fig. 1C). For further elucidation, the superimposed structure of the modeled SiLTPI.5 and a variety of known structures were built; the results showed that they were different in the outer region at loop-4 through the C-terminal part (Fig. 1D).

SiLTPII.1 contained 96 amino acid residues, (a mature protein of 68 amino acids and a putative signal peptide of 28 amino acids), with a pI of 9.44 and a mature mass of 7.26 kDa. The 3D structure of SiLTPII.1 had a highest GMQE score of 0.68. Sequence comparison revealed that the SiLTPII.1 of sesame showed relatively high similarity to the *T. aestivum* nsLTP compared to that of *O. sativa*, with a sequence identity of 44.78% and a QMEANDisCo Global score of  $0.68 \pm 0.11$ . The quality of the constructed model showed that 98.46% of the amino acids were in the most favorable region, with a MolProbity score of 0.80. The nsLTPII sequence alignments of known structures, including the X-ray diffracted structure of *T. aestivum*

(a model template) and NMR spectroscopy of *O. sativa* (PDB code: 1L6H; Samuel et al., 2002) were performed and the results are shown in Fig. 2A. Despite limited studies on nsLTPII, a representative of nsLTPII sequence alignment revealed common conserved amino acids and the X position of the -CXC- motif was leucine, which was different to the nsLTPII of wheat and rice, wherein phenylalanine replaced leucine. However, an amino acid with a hydrophobic side chain was generally seen in the nsLTPII of this motif, while nsLTPI exhibited a hydrophilic residue which may govern the cysteine pairing and consequently directly protein folding (Samuel et al., 2002). The predicted 3D structure of SiLTPII.1 is presented in Fig. 2B, consisting of five helices, an N-terminal  $3_{10}$ -helix, a C-terminal with a short polyproline type II and four disulfide bridges. Fig. 2C represents the hydrophobicity of SiLTPII.1, exhibiting a closed form, as observed in SiLTPI.5. The modeled SiLTPII.1 had similar conformation as the wheat nsLTPII but with several different structures to the rice nsLTPII (Fig. 2D). The rice nsLTPII was the first published structure using the NMR technique with an 813 distance, 30 hydrogen bonds and 19 dihedral angle constraints (Samuel et al., 2002). Liganded wheat nsLTPII from NMR was also reported by Pons et al. (2003). Nevertheless, the folding of these two structures were substantially different. Thus, in the current study the X-ray structure was used of the wheat nsLTPII with high diffraction resolution as a template for the SiLTPII.1 model to provide a reasonable structure.

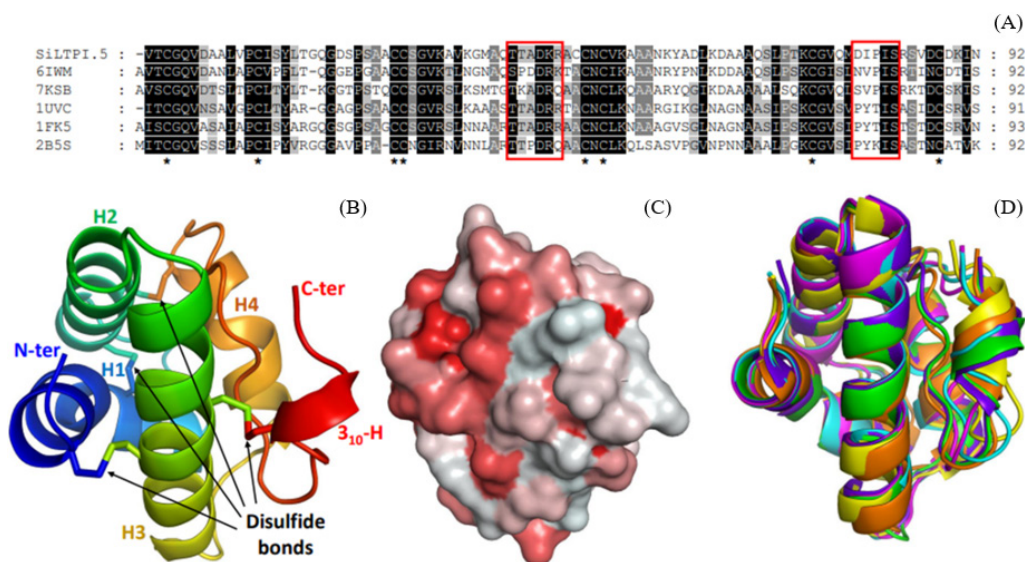


**Fig. 1** Spatial structure of SiLTPI.5: (A) amino acid sequence alignment of SiLTPI.5, *S. melongena* (PDB code: 6IWM), *A. chinensis* (PDB code: 7KSB), *O. sativa* (PDB code: 1UVC), *Z. mays* (PDB code: 1FK5) and *P. persica* (PDB code: 2B5S), where stars indicate conserved Cys residues and red boxes show conserved motifs of T/SXXDR/K and PYXIS; (B) ribbon diagram showing overall structure of SiLTPI.5; (C) hydrophobic patches on surface of SiLTPI.5; (D) superimposition of SiLTPI.5 structure (green), *S. melongena* (purple), *A. chinensis* (orange), *O. sativa* (magenta), *Z. mays* (cyan) and *P. persica* (yellow)



**Table 1** Molecular docking analysis of SiLTPI.5

Ligand	Binding energy (kcal/mol)	Amino acid residues forming hydrogen bonds with ligand	Amino acid with hydrophobic side chains at binding site within 4 Å
Decanoic acid	-3.27	Q68, P71, T72	A67, M78, I80, I82
Lauric acid	-3.50	Q68, P71, T72	M78, I80, I82
Myristic acid	-3.45	N92	A67, M78, I80, I82, I91
Palmitic acid	-3.56	T72, Q77	A67, V76, M78, I80, I82
Stearic acid	-3.63	Q68, T72	A67, M78, I80, I82, I91
Palmitoleic acid	-3.45	K45, D79	A67, M78, I80, I82
Oleic acid	-4.27	D79, N92	A67, M78, I80, I82, I91
Ricinoleic acid	-3.73	V76, Q77, M78	V76, M78, I80, I82
Elaidic acid	-3.75	D79	V76, M78, I80, I82
OEA	-3.85	Q68, T72, I82	M78, I80, I82, I91
Linoleic acid	-3.60	-	A67, V76, M78, I80, I82
Linolenic acid	-4.51	N92	V76, M78, I80, I91
octacosan-1-ol	-2.04	Q68	M78, I80, I82
PPC	-3.80	Q68, T72, V76, M78, P81, I82	V76, M78, I80, I82
LLPC	-3.05	Q68	V76, M78, I80, I82
DLPC	-2.61	Q68, Q77, M78, I82	A67, M78, I80, I82
MLPG	-2.07	Q68, M78, I80, S83	V76, M78, I80, I82, V86
MLPC	-3.58	A67, Q68, I82	A67, M78, I80, I82, I91
Phytosphingosine	-3.56	Q68, I82, S83	M78, I80, I82, I91
Prostaglandin B2	-5.86	A67, Q68, T72	A67, M78, I80, I82
(Ergo)sterol	-6.92	-	V76, M78, I80, I82, V86
Jasmonic acid	-5.09	Q68, P71, T72, I82	A67, M78, I80, I82

OEA = (12E)-10-oxooctadec-12-enoic acid; PPC = phosphatidylcholine; LLPC = 1-lauroyl-2-hydroxy-sn-glycero-3-phosphocholine; DLPC = 1-dodecanoyl-sn-glycero-3-phosphocholine; MLPG = 1-myristoyl-2-hydroxy-sn-glycero-3-[phospho-rac-(1-glycerol)]; MLPC = (1-myristoyl-glycerol-3-YL) phosphonylcholine

**Table 2** Molecular docking analysis of SiLTPII.1

Ligand	Binding energy (kcal/mol)	Amino acid residues forming hydrogen bonds with ligand	Amino acid with hydrophobic side chains at binding site within 4 Å
Decanoic acid	-3.97	-	L6, L8, A12, I15, L45, F48, I49
Lauric acid	-3.92	-	L6, L8, A12, I15, L45, F48, I49
Myristic acid	-3.86	-	L6, L8, A12, I15, L45, F48, I49
Palmitic acid	-4.06	-	L6, L8, A12, I15, L45, F48
Stearic acid	-4.01	S9	L6, L8, A12, I15, L45, F48, I49
Palmitoleic acid	-3.77	-	L6, L8, A12, I15, L45, F48
Oleic acid	-4.05	N44	L6, L8, I15, L45, F48, I49
Ricinoleic acid	-4.15	R33, Q38	L36
Elaidic acid	-3.71	S9	L6, L8, A12, I15, L45, F48, I49
OEA	-3.75	-	L6, L8, I15, L45, F48, I49
Linoleic acid	-4.06	-	L6, L8, A12, I15, L45, F48
Linolenic acid	-4.67	-	L6, L8, I15, L45, F48, I49
octacosan-1-ol	-0.29	N44	A12, A14, L45, F48
PPC	-2.92	P5	L6, L8, A12, I15, L45, F48, I49
LLPC	-1.14	-	L8, A12, I15, L45, F48
DLPC	-1.47	L8	L8, A12, I15, L45, F48
MLPG	3.36	P5, S9	L6, L8, A12, L45, I49
MLPC	-1.46	K47, K50, P52	M40, Y65
Phytosphingosine	-2.92	-	L6, L8, A12, I15, L45, F48
Prostaglandin B2	-4.62	-	L6, L8, A12, I15, L45, F48, I49
(Ergo)sterol	-6.87	Q38	L36
Jasmonic acid	-5.71	-	L6, L8, A12, I15, L45, F48, I49

OEA = (12E)-10-oxooctadec-12-enoic acid; PPC = phosphatidylcholine; LLPC = 1-lauroyl-2-hydroxy-sn-glycero-3-phosphocholine; DLPC = 1-dodecanoyl-sn-glycero-3-phosphocholine; MLPG = 1-myristoyl-2-hydroxy-sn-glycero-3-[phospho-rac-(1-glycerol)]; MLPC = (1-myristoyl-glycerol-3-YL) phosphonylcholine

Structural stability over the simulation time was demonstrated compared to the initial protein backbones. For SiLTPI.5, the root-mean-square-deviation (RMSD) values were 1.5 Å during 200 ns, whereas for SiLTPII.1, the RMSD values were not constant from the beginning of the simulation times until 100–200 ns, when they reached 3.0 Å (Fig. S1). These results indicate that the studied system of SiLTPI.5 was more stable than for SiLTPII.1. In addition, the fluctuation of protein residues upon ligand binding was investigated based on the root-mean-square-fluctuation (RMSF). During the MD simulation trajectory, the RMSF during 1–100 ns of SiLTPI.5 had somewhat fewer fluctuations than during 100–200 ns (Fig. S2). These results showed that the ligand was bound to the protein for a particular time, then movement occurred within the binding regions. For SiLTPII.1, the amino acid residues 30–47 were more fluctuated during 1–200 ns than other positions (Fig. S3). This result was consistent with docking analysis, for which L36 and Q38 were formed hydrophobic and hydrogen bonding, respectively. The interaction energy between proteins at 5.0 Å around the lipid was investigated using the NAMD energy calculations and the results are shown in Table 3. The interaction energy values for SiLTPI.5 and SiLTPII.1 were -19.832 kcal/mol and -25.539 kcal/mol, respectively, with rather high van der Waals energy than

electrostatic energy. The complexes were more stabilized via hydrogen bonds as found during the simulation (Tables S1 and S2), correlating with the docking results, hence indicating that the binding between SiLTPIs and (ergo)sterol could be maintained and stabilized via hydrophobic force and hydrogen bonding. The position and orientation of (ergo)sterol from the docking and MD simulation were slightly different; however, they were bound with the protein in the same region around the C-terminal part (Fig. 3), suggesting that this region might be the most favorite region of the protein-ligand interaction for plant nsLTPs. To date, X-ray crystal and NMR structures of nsLTPs in complex with (ergo)sterol have not been deposited in the PDB database. *In vitro* and *in vivo* studied of Wheat LTPI, according to Buhot et al. (2001), was unable to capture phytosterols. The sterol molecule could not fit in the hydrophobic cavity of nsLTP1 due to its rigidity (Samuel et al., 2022). The current findings revealed a surprising distinction. At the hydrophobic cavity, SiLTPI.5 could be maintained and stabilized (ergo)sterol, which might be because of the difference at loop-4 through the C-terminal part and amino acids in the lipid-binding at PYXIS motif. According to Fig. 1A, sesame exhibits DIPIS which mean an amino acid with a negatively charged and more hydrophobic side chain may have an impact on the binding of (ergo)sterols in this motif. To identify the amino acids that are crucial for lipid binding, a site-directed mutagenesis study should be conducted. In the case of nsLTPII, the hydrophobic cavity of rice nsLTPII, which is smaller than that of rice nsLTPI, was able to accommodate the ergosterol molecule without substantially changing the tertiary protein structure (Cheng et al., 2004a). This finding is in line with the current studied.

**Table 3** Estimates of SiLTPIs-(ergo)sterol interaction energies

System	Electrostatic energy (kcal/mol)	Van der Waals energy (kcal/mol)	Interaction energy (kcal/mol)
SiLTPI.5-(ergo)sterol	-5.05858	-14.7729	-19.8315
SiLTPII.1-(ergo)sterol	-2.13706	-23.4017	-25.5388

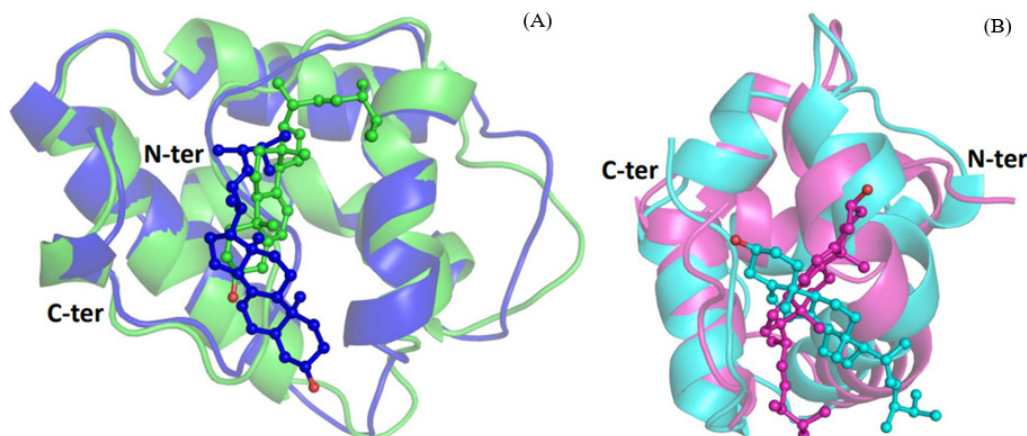


**Fig. 3** Superimposition of docked SiLTPIs and MD simulation: (A) docked SiLTPI.5 (green) and SiLTPI.5 from molecular dynamics (MD) simulation (blue); (B) docked SiLTPII.1 (magenta) and SiLTPII.1 from MD simulation (cyan), where (ergo)sterol ligand shown using ball and stick presentation

### Transcriptional levels of *SiLTPI.5* and *SiLTPII.1* responding to abiotic stresses

It is well known that plant growth and development are limited by environmental stresses (Ahanger et al., 2017; Zhang et al., 2020). LTPs play roles in responding to various stresses and repairing stress-induced damage in membranes (Hairat et al., 2018). To validate the abiotic stress responses in the plant cell, qRT-PCR was used to measure the level of the *SiLTPI.5* and *SiLTPII.1* expressions in sesame (Fig. 4). In the current study, under NaCl treatment, the expression of the *SiLTPI.5* and *SiLTPII.1* genes of white and black sesame

were considerably upregulated at the 150 mM concentration except for *SiLTPII.1* in white sesame. In the chilling treatment, *SiLTPI.5* was upregulated at 4°C, 15°C and 20°C in white sesame, while black sesame was substantially upregulated at all chilling treatment temperatures. The upregulation of *SiLTPII.1* was induced at 20°C for black sesame. Notably, at 10°C, the *SiLTPs* gene was downregulated, suggesting that this might be a critical temperature for sesame to protect the cells by a process to acquire cold tolerance through the gradual exposure to low temperature, known as cold acclimation (Shen et al., 2021). After the heat treatment, both genes in the black sesame were upregulated in response to all temperature treatments.

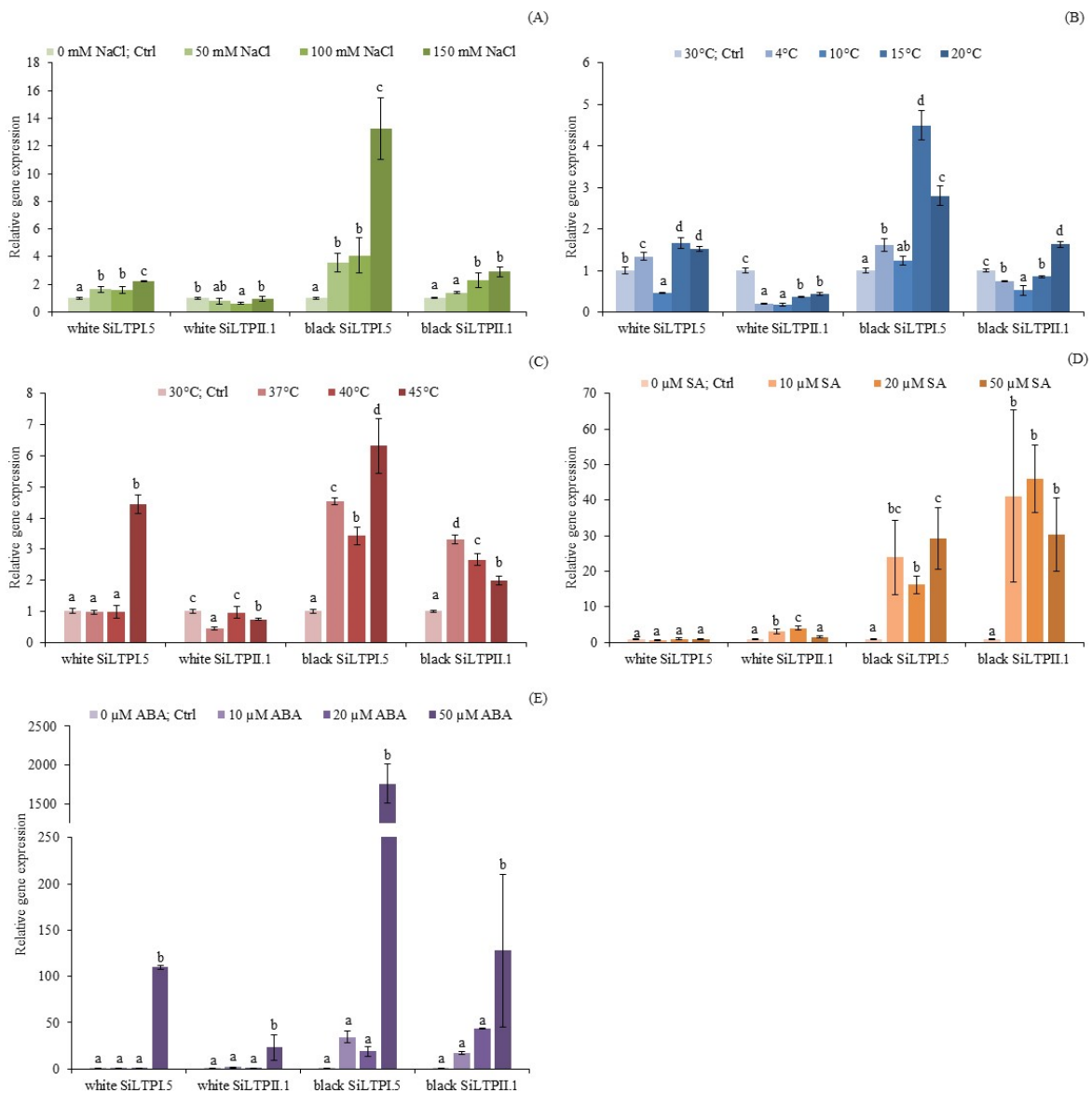


**Fig. 4** Relative gene expressions of *SiLTPI.5* and *SiLTPII.1* under: (A) NaCl; (B) chilling; (C) heat; (D) salicylic acid (SA); (E) and abscisic acid (ABA) treatments, where error bars indicate mean  $\pm$  SD and different lowercase letters above columns indicate significant differences at  $p < 0.05$ .

In contrast, downregulation was observed for *SiLTPII.1* in white sesame at 37°C. However, when the temperature increased to 40°C and 45°C, the *SiLTPIs* of white sesame gradually upregulated. Following the SA and ABA treatments, black sesame showed a higher magnitude of relative expression fold than from salinity, chilling and heating, especially in the ABA treatment. The transcript levels of *SiLTPI.5* in white sesame after the SA treatment were not different from the control condition, while both genes of black sesame were upregulated when exposed to 10–50 µM of SA. The expression level of *SiLTPII.1* was enhanced and significantly different among all the SA treatments for both genotypes, except for white sesame at 50 µM concentration. Finally, after the ABA treatment, *SiLTPI.5* and *SiLTPII.1* were significantly upregulated at 50 µM for both genotypes. Notably, despite the fact that both the transcript levels for the genes in white and black sesame tended to increase, black sesame demonstrated higher relative gene expression than white sesame. This might have been due to the black sesame utilizing nsLTPs more effectively as one of its defense mechanisms than white sesame, with white sesame using a different strategy to defend the cell from abiotic stresses. Overall, it can be concluded that expression of the *SiLTPI.5* and *SiLTPII.1* genes was significantly affected by salinity, chilling, heating, SA and ABA, thus suggesting that these genes play a crucial role in the protective mechanisms established by sesame cells against abiotic stresses.

In conclusion, the spatial structures were successfully developed of *SiLTPI.5* and *SiLTPII.1* using the SWISS-MODEL server. The overall structure of *SiLTPI.5* consisted of four helices, four loops, a long C-terminal with a  $3_{10}$ -helix and four disulfide bonds, while *SiLTPII.1* consisted of five helices, an N-terminal  $3_{10}$ -helix, a C-terminal with a short polyproline type II and four disulfide bridges. Both structures represented a hydrophobic cavity in a closed form. *SiLTPI.5* and *SiLTPII.1* had strong binding energies with lipid molecules. The highest energy was found with (ergo)sterol followed by prostaglandin B2 for *SiLTPI.5* and jasmonic acid for *SiLTPII.1*. The *SiLTP*-lipids interactions were stabilized via conserved amino acid with hydrophobic side chains around the binding region, together with some hydrogen bonds between the protein and ligand. Molecular docking and MD simulations validated that the C-terminal region as possibly the most important region of the protein-ligand interaction for plant nsLTPs. Finally, the *SiLTPI.5* and *SiLTPII.1* genes were upregulated when sesame was treated with salinity, chilling, heating, SA and ABA, suggesting that these genes play a crucial role in stress responses.

---

## Conflict of Interest

The authors declare that there are no conflicts of interest.

---

## Acknowledgements

We are grateful to Prof. Dr. James R. Ketudat-Cairns for his suggestions in the experiments and to Prof. Dr. Uthairat Na-Nakorn for her valuable comments on this manuscript. This research was supported by the Kasetsart University Research and Development Institute (KURDI), Bangkok, Thailand (R-M 33.60) and partially supported by the Faculty of Science at Sriracha, Kasetsart University at Sriracha Campus.

---

## References

- Adeyanju, M.M., Saheed, I.A., Oyelekan, O.I., et al. 2022. *Sesamum indicum* diet prevents hyperlipidemia in experimental rats. *Food Chem.* 4: 100092. doi.org/10.1016/j.fochms.2022.100092
- Ahanger, M.A., Akram, N.A., Ashraf, M., Alyemeni, M.N., Wijaya, L., Ahmad, P. 2017. Plant responses to environmental stresses-from gene to biotechnology. *AoB Plants* 9: plx025. doi.org/10.1093/aobpla/plx025
- Akhiyarova, G.R., Finkina, E.I., Ovchinnikova, T.V., Veselov, D.S., Kudoyarova, G.R. 2020. Role of pea LTPs and abscisic acid in salt-stressed roots. *Biomolecules* 10: 15. doi.org/10.3390/biom10010015
- Baiya, S., Pengthaisong, S., Kitjaruwankul, S., Cairns, J.R.K. 2021. Structural analysis of rice Os4BGlu18 monolignol β-glucosidase. *PLoS One* 16: e0241325. doi.org/10.1371/journal.pone.0241325
- Boutrot, F., Chantret, N., Gautier, M.-F. 2008. Genome-wide analysis of the rice and arabidopsis *non-specific lipid transfer protein (nsLtp)* gene families and identification of wheat *nsLtp* genes by EST data mining. *BMC Genom.* 9: 86. doi.org/10.1186/1471-2164-9-86
- Buhot, N., Douliez, J.P., Jacquemard, A., et al. 2001. A lipid transfer protein binds to a receptor involved in the control of plant defence responses. *FEBS Lett.* 509: 27–30. doi.org/10.1016/S0014-5793(01)03116-7
- Carvalho, A.d.O., Gomes, V.M. 2007. Role of plant lipid transfer proteins in plant cell physiology—A concise review. *Peptides* 28: 1144–1153. doi.org/10.1016/j.peptides.2007.03.004
- Chen, Y., Ma, J., Zhang, X., et al. 2017. A novel non-specific lipid transfer protein gene from sugarcane (NsLTPs), obviously responded to abiotic stresses and signaling molecules of SA and MeJA. *Sugar Tech* 19: 17–25. doi.org/10.1007/s12355-016-0431-4
- Cheng, C.S., Samuel, D., Liu, Y.J., Shyu, J.C., Lai, S.M., Lin, K.-F., Lyu, P.-C. 2004a. Binding mechanism of nonspecific lipid transfer proteins and their role in plant defense. *Biochemistry* 43: 13628–13636. doi.org/10.1021/bi048873j
- Cheng, H.C., Cheng, P.T., Peng, P., Lyu, P.C., Sun, Y.J. 2004b. Lipid binding in rice nonspecific lipid transfer protein-I complexes from *Oryza sativa*. *Protein Sci.* 13: 2304–2315. doi.org/10.1110/ps.04799704

- Choi, A.M., Lee, S.B., Cho, S.H., Hwang, I., Hur, C.G., Suh, M.C. 2008. Isolation and characterization of multiple abundant lipid transfer protein isoforms in developing sesame (*Sesamum indicum* L.) seeds. *Plant Physiol. Biochem.* 46: 127–139. doi.org/10.1016/j.plaphy.2007.10.003
- Cubells-Baeza, N., Gómez-Casado, C., Tordesillas, L., et al. 2017. Identification of the ligand of Pru p 3, a peach LTP. *Plant Mol. Biol.* 94: 33–44. doi.org/10.1007/s11103-017-0590-z
- Cuevas-Zuviria, B., Garrido-Arandia, M., Díaz-Perales, A., Pacios, L.F. 2019. Energy landscapes of ligand motion inside the tunnel-like cavity of lipid transfer proteins: The case of the Pru p 3 allergen. *Int. J. Mol. Sci.* 20: 1432. doi.org/10.3390/ijms20061432
- Darden, T., York, D., Pedersen, L. 1998. Particle mesh Ewald: an N log (N) method for Ewald sums in large systems. *J. Chem. Phys.* 98: 10089–10092. doi.org/10.1063/1.464397
- Dossou, S.S.K., Fang-tao, X., Dossa, K., Rong, Z., Ying-zhong, Z., Lin-hai, W. 2023. Antioxidant lignans sesamin and sesamol in sesame (*Sesamum indicum* L.): A comprehensive review and future prospects. *J. Integr. Agric.* 22: 14–30. doi.org/10.1016/j.jia.2022.08.097
- Edgar, R.C. 2004. MUSCLE: Multiple sequence alignment with high accuracy and high throughput. *Nucleic Acids Res.* 32: 1792–1797. doi.org/10.1093/nar/gkh340
- Edstam, M.M., Viitanen, L., Salminen, T.A., Edqvist, J. 2011. Evolutionary history of the non-specific lipid transfer proteins. *Mol. Plant* 4: 947–964. doi.org/10.1093/mp/ssr019
- Finkina, E.I., Melnikova, D.N., Bogdanov, I.V., Ovchinnikova, T.V. 2016. Lipid transfer proteins as components of the plant innate immune system: Structure, functions, and applications. *Acta Naturae* 8: 47–61. doi.org/10.32607/20758251-2016-8-2-47-61
- Gangadhar, B.H., Sajeesh, K., Venkatesh, J., Baskar, V., Abhinandan, K., Yu, J.W., Prasad, R., Mishra, R.K. 2016. Enhanced tolerance of transgenic potato plants over-expressing non-specific lipid transfer protein-1 (StnsLTP1) against multiple abiotic stresses. *Front. Plant Sci.* 7: 1228. doi.org/10.3389/fpls.2016.01228
- Gonzalez-Klein, Z., Cuevas-Zuviria, B., Wangorsch, A., et al. 2021. The key to the allergenicity of lipid transfer protein (LTP) ligands: A structural characterization. *BBA Mol. Cell Biol. L.* 1866: 158928. doi.org/10.1016/j.bbali.2021.158928
- Gupta, A., Bano, A., Rai, S., Mishra, R., Singh, M., Sharma, S., Pathak, N. 2022. Mechanistic insights of plant-microbe interaction towards drought and salinity stress in plants for enhancing the agriculture productivity. *Plant Stress* 4: 100073. doi.org/10.1016/j.stress.2022.100073
- Hairat, S., Baranwal, V.K., Khurana, P. 2018. Identification of *Triticum aestivum* nsLTPs and functional validation of two members in development and stress mitigation roles. *Plant Physiol. Biochem.* 130: 418–430. doi.org/10.1016/j.plaphy.2018.07.030
- Han, G.W., Lee, J.Y., Song, H.K., et al. 2001. Structural basis of non-specific lipid binding in maize lipid-transfer protein complexes revealed by high-resolution X-ray crystallography. *J. Mol. Biol.* 308: 263–278. doi.org/10.1006/jmbi.2001.4559
- Hoh, F., Pons, J.L., Gautier, M.F., de Lamotte, F., Dumas, C. 2005. Structure of a liganded type 2 non-specific lipid-transfer protein from wheat and the molecular basis of lipid binding. *Acta Cryst.* 61: 397–406. doi.org/10.1107/S0907444905000417
- Hoover, W.G., 1985. Canonical dynamics: Equilibrium phase-space distributions. *Phys. Rev. A.* 31: 1695–1697. doi.org/10.1103/physreva.31.1695
- Huang, J., Rauscher, S., Nawrocki, G., Ran, T., Feig, M., Groot, B.L.d., Grubmüller, H., MacKerell, A.D.Jr. 2016. CHARMM36m: An improved force field for folded and intrinsically disordered proteins. *Nat. Methods.* 14: 71–73. doi.org/10.1038/nmeth.4067
- Humphrey, W., Dalke, A., Schulten, K. 1996. VMD: Visual molecular dynamics. *J. Mol. Graph.* 14: 33–38. doi.org/10.1016/0263-7855(96)00018-5
- Jorgensen, W.L., Chandrasekhar, J., Madura, J.D., Impey, R.W., Klein, M.L. 1983. Comparison of simple potential functions for simulating liquid water. *J. Chem. Phys.* 79: 926–935. doi.org/10.1063/1.445869
- Khuimphukhieo, I., Khaengkhan, P., Sarepoua, E. 2020. Inheritance, heritability and association of agronomic traits and sesamin and sesamol contents in sesame (*Sesamum indicum* L.). *Agr. Nat. Resour.* 54: 439–446. doi.org/10.34044/j.anres.2020.54.4.13
- Korkmaz, A., Değer, Ö., Szafranska, K., Köklü, Ş., Karaca, A., Yakupoğlu, G., Kocacina, F. 2021. Melatonin effects in enhancing chilling stress tolerance of pepper. *Sci. Hortic.* 289: 110434. doi.org/10.1016/j.scienta.2021.110434
- Liu, F., Zhang, X., Lu, C., Zeng, X., Li, Y., Fu, D., Wu, G. 2015. Non-specific lipid transfer proteins in plants: Presenting new advances and an integrated functional analysis. *J. Exp. Bot.* 66: 5663–5681. doi.org/10.1093/jxb/erv313
- Ma, X., Wang, Z., Zheng, C., Liu, C. 2022. A comprehensive review of bioactive compounds and processing technology of sesame seed. *Oil Crop Sci.* 7: 88–94. doi.org/10.1016/j.oecsci.2022.05.003
- Ma, Y., Dias, M.C., Freitas, H. 2020. Drought and salinity stress responses and microbe-induced tolerance in plants. *Front. Plant Sci.* 11: 591911. doi.org/10.3389/fpls.2020.591911
- Madni, Z.K., Tripathi, S.K., Salunke, D.M. 2020. Structural insights into the lipid transfer mechanism of a non-specific lipid transfer protein. *Plant J.* 102: 340–352. doi.org/10.1111/tpj.14627
- Melnikova, D.N., Bogdanov, I.V., Ignatova, A.A., Ovchinnikova, T.V., Finkina, E.I. 2020. New insights into ligand binding by plant lipid transfer proteins: A case study of the lentil Lc-LTP2. *Biochem. Biophys. Res. Commun.* 528: 39–45. doi.org/10.1016/j.bbrc.2020.04.139
- Missaoui, K., Gonzalez-Klein, Z., Pazos-Castro, D., Hernandez-Ramirez, G., Garrido-Arandia, M., Brini, F., Diaz-Perales, A., Tome-Amat, J. 2022. Plant non-specific lipid transfer proteins: An overview. *Plant Physiol. Biochem.* 171: 115–127. doi.org/10.1016/j.plaphy.2021.12.026
- Namiki, M. 2007. Nutraceutical functions of sesame: A review. *Crit. Rev. Food Sci. Nutr.* 47: 651–673. doi.org/10.1080/10408390600919114
- O'Malley, A., Pote, S., Giangrieco, I., Tuppo, L., Gawlicka-Chruszcz, A., Kowal, K., Ciardiello, M.A., Chruszcz, M. 2021. Structural characterization of act c 10.0101 and pun g 1.0101—allergens from the non-specific lipid transfer protein family. *Molecules* 26: 256. doi.org/10.3390/molecules26020256
- Østergaard, J., Vergnolle, C., Schoentgen, F., Kader, J.C. 1993. Acyl-binding/lipid transfer proteins from rape seedlings, a novel category of proteins interacting with lipids. *BBA Lipid Lipid Met.* 1170: 109–117. doi.org/10.1016/0005-2760(93)90059-I

- Pasquato, N., Berni, R., Folli, C., Folloni, S., Cianci, M., Pantano, S., Helliwell, J.R., Zanotti, G. 2006. Crystal structure of peach Pru p 3, the prototypic member of the family of plant non-specific lipid transfer protein pan-allergens. *J. Mol. Biol.* 356: 684–694. doi.org/10.1016/j.jmb.2005.11.063
- Pons, J.L., de Lamotte, F., Gautier, M.F., Delsuc, M.A. 2003. Refined solution structure of a liganded type 2 wheat nonspecific lipid transfer protein. *J. Biol. Chem.* 278: 14249–14256. doi.org/10.1074/jbc.M211683200
- Phillips, J.C., Braun, R., Wang, W., et al. 2008. Scalable molecular dynamics with NAMD. *J. Comput. Chem.* 26: 1781–1802. doi.org/10.1002/jcc.20289
- Qin, F., Kazuo, S., Kazuo, Y.S. 2011. Achievement and challenges in understanding plant abiotic stress responses and tolerance. *Plant Cell Physiol.* 52: 1569–1582. doi.org/10.1093/pcp/pcr106
- Rao, X., Huang, X., Zhou, Z., Lin, X. 2013. An improvement of the 2<sup>Δ</sup>(-delta delta CT) method for quantitative real-time polymerase chain reaction data analysis. *Biostat. Bioinforma. Biomath.* 3: 71–85.
- Rizvi, S.M., Shakil, S., Haneef, M., 2013. A simple click by click protocol to perform docking: AutoDock 4.2 made easy for non-bioinformaticians. *EXCLI J.* 12: 835–857.
- Ryckaert, J.P., Ciccotti, G., Berendsen, H.J.C. 1977. Numerical integration of the cartesian equations of motion of a system with constraints: molecular dynamics of n-alkanes. *J. Comput. Phys.* 23: 327–341. doi.org/10.1016/0021-9991(77)90098-5
- Safi, H., Saibi, W., Alaoui, M.M., Hmyene, A., Masmoudi, K., Hanin, M., Brini, F. 2015. A wheat lipid transfer protein (TdLTP4) promotes tolerance to abiotic and biotic stress in *Arabidopsis thaliana*. *Plant Physiol. Biochem.* 89: 64–75. doi.org/10.1016/j.plaphy.2015.02.008
- Salminen, T.A., Blomqvist, K., Edqvist, J. 2016. Lipid transfer proteins: Classification, nomenclature, structure, and function. *Planta* 244: 971–997. doi.org/10.1007/s00425-016-2585-4
- Samuel, D., Liu, Y.J., Cheng, C.S., Lyu, P.C. 2002. Solution structure of plant nonspecific lipid transfer protein-2 from rice (*Oryza sativa*). *J. Biol. Chem.* 277: 35267–35273. doi.org/10.1074/jbc.M203113200
- Scheurer, S., Schülke, S. 2018. Interaction of non-specific lipid-transfer proteins with plant-derived lipids and its impact on allergic sensitization. *Front. Immunol.* 9: 1389. doi.org/10.3389/fimmu.2018.01389
- Shenkarev, Z.O., Melnikova, D.N., Finkina, E.I., et al. 2017. Ligand binding properties of the lentil lipid transfer protein: Molecular insight into the possible mechanism of lipid uptake. *Biochemistry* 56: 1785–1796. doi.org/10.1021/acs.biochem.6b01079
- Shen, Z.J., Qin, Y.Y., Luo, M.R., Li, Z., Ma, D.N., Wang, W.-H., Zheng, H.-L. 2021. Proteome analysis reveals a systematic response of cold-acclimated seedlings of an exotic mangrove plant *Sonneratia apetala* to chilling stress. *J. Proteom.* 248: 104349. doi.org/10.1016/j.jprot.2021.104349
- Shi, Z., Wang, Z., Xu, H., Tian, Y., Li, X., Bao, J.-K., Sun, S., Yue, B. 2013. Modeling, docking and dynamics simulations of a non-specific lipid transfer protein from *Peganum harmala* L. *Comput. Biol. Chem.* 47: 56–65. doi.org/10.1016/j.compbiolchem.2013.07.001
- Song, S., You, J., Shi, L., et al. 2021. Genome-wide analysis of nsLTP gene family and identification of *SiLTPs* contributing to high oil accumulation in sesame (*Sesamum indicum* L.). *Int. J. Mol. Sci.* 22: 5291. doi.org/10.3390/ijms22105291
- Suh, M.C., Kim, M.J., Hur, C.G., Bae, J.M., Park, Y.I., Chung, C.-H., Kang, C.-W., Ohlrogge, J.B. 2003. Comparative analysis of expressed sequence tags from *Sesamum indicum* and *Arabidopsis thaliana* developing seeds. *Plant Mol. Biol.* 52: 1107–1123. doi.org/10.1023/b:plan.0000004304.22770.e9
- Wahid, A., Gelani, S., Ashraf, M., Foolad, M.R. 2007. Heat tolerance in plants: An overview. *Environ. Exp. Bot.* 61: 199–223. doi.org/10.1016/j.envexpbot.2007.05.011
- Wang, F., Zang, X., Kabir, M.R., et al. 2014. A wheat lipid transfer protein 3 could enhance the basal thermotolerance and oxidative stress resistance of *Arabidopsis*. *Gene* 550: 8–26. doi.org/10.1016/j.gene.2014.08.007
- Wani, S.H., Kumar, V., Shriram, V., Sah, S.K. 2016. Phytohormones and their metabolic engineering for abiotic stress tolerance in crop plants. *Crop J.* 4: 162–176. doi.org/10.1016/j.cj.2016.01.010
- Yang, Y., Li, P., Liu, C., Wang, P., Cao, P., Ye, X., Li, Q. 2022. Systematic analysis of the non-specific lipid transfer protein gene family in *Nicotiana tabacum* reveal its potential roles in stress responses. *Plant Physiol. Biochem.* 172: 33–47. doi.org/10.1016/j.plaphy.2022.01.002
- Zhang, H., Zhao, Y., Zhu, J. 2020. Thriving under stress: How plants balance growth and the stress response. *Dev. Cell.* 55: 529–543. doi.org/10.1016/j.devcel.2020.10.012
- Zhang, P.G., Hou, Z.H., Chen, J., et al. 2022. The non-specific lipid transfer protein GmLtpI.3 is involved in drought and salt tolerance in soybean. *Environ. Exp. Bot.* 196: 104823. doi.org/10.1016/j.envexpbot.2022.104823